The Crystalline Structure of Amylose Triacetate I. A Stereochemical Approach

A. Sarko and R. H. Marchessault

Contribution from the Cellulose Research Institute and Chemistry Department, State University College of Forestry, Syracuse, New York. *Received July 17, 1967*

Abstract: The crystal structure of oriented amylose triacetate I, previously shown to consist of helical chains with 14 monomer residues in three turns, has been determined by combined X-ray diffraction and stereochemical model analysis. Each possible helix model consistent with the X-ray data was characterized by a nonbonded potential energy. Assuming a *C1* conformation for the glucopyranose ring, the analysis led to selection of a left-handed helix with fully specified conformation in terms of acetate substituents. The chain-packing problem was also solved by combining potential energy criteria and diffracted intensity calculations. The most probable interchain packing in terms of the parallel and antiparallel arrangement was sought by determining the chain packing resulting in the least number of short nonbonded interatomic contacts. Simultaneously the best match of theoretical and observed intensities was sought. The results clearly favored the antiparallel arrangement in the pseudo-hexagonal unit cell.

In recent years a stereochemical approach to the conformation of linear polymers has been developing.[1] Of the large number of theoretically possible conformations which a polymer can adopt through rotations about single bonds, only a minority will satisfy the elementary stereochemical criterion of minimum contact distance between atoms. Thus, simply on the basis of short van der Waals contact between nonbonded atoms, one is able to decide whether a given conformation is plausible. With a high-speed computer and a reasonable scheme for generating and varying the model, the range of tenable conformations can be determined within a relatively short time.

The ultimate success of this approach is judged by comparing results with experimental data. This is most conveniently done by comparing observed X-ray intensities with those calculated from the predicted structure. As is well known, the intensity of X-ray reflections is very sensitive to changes in atomic positions. In effect, this procedure also makes possible a further refinement of the predicted structure in that the range of plausible conformations is systematically explored for the best match of calculated and observed intensities. This is not possible by simple visual exploration of a solid model.

The stereochemical approach has been applied in varying degrees of refinement to a number of polymers: cellulose,[2] stereoregular vinyl polymers,[3] and polypeptides.[1] It is not illogical to speculate that if the structure of one polymer within a given class were successfully predicted *via* this method, the same procedure could be used for other members of the class of known chemical structure. This would be of special value where experimental data are either not available or of poor quality, as is often the case with polysaccharides.

With this in mind, a conformational study of the crystal structure of amylose triacetate was undertaken. The objective of this study was to develop a method which would assist in the interpretation of polysaccharide X-ray diffractograms. Amylose triacetate was selected for study because (a) the X-ray fiber diagram is exceptionally clear compared to most other polysaccharides and definitely indicates a helical conformation,[4] and (b) the information and methods would serve immediately in the study of the crystal structure and texture of amylose and the starch granule, for which only poor experimental data are available.

In a previous communication, we reported that the helix of amylose triacetate I was of nonintegral type and consisted of 14 monomer residues per three turns of the helix.[4] This was deduced from a comparison of the distribution of intensity in the diffractogram with that predicted by the molecular transform of the helix. Although all reflections fell on clearly resolved layer lines, the separation of layers in reciprocal space was not constant and could not be accounted for by a single fiber repeat. While this analysis defined the helix in its general outline, other information such as the chirality of the helix, relative orientation of neighboring repeat units, conformation of acetate substituents, and intermolecular packing were not readily derivable from the X-ray data. Subsequent work with better oriented and better crystallized samples has produced X-ray diagrams with well-resolved reflections from which intensity data could be derived.

Experimental Section

Preparation of Samples. The best sample for X-ray purposes was obtained by starting from an experimental corn amylose (code NRRL, 14SSP) supplied by the Regional Laboratories of the U. S. Department of Agriculture, Peoria, Ill. The physical characteristics of this sample are given in Table I. The triacetate was prepared according to the method of Jeanes and Jones[5] and was made into a film by evaporation of a 5% chloroform solution. The characteristics of the triacetate are likewise described in Table I. Strips of the film, 20 mm long, 3 mm wide, and approximately 40 μ thick, were stretched in glycerol at 160° to an extension of at least 500%. The stretched films were washed free of glycerol with

(1) (a) G. N. Ramachandran in "Structural Chemistry and Molecular Biology," A. Rich, and N. Davidson, Ed., W. H. Freeman and Co., San Francisco, Calif., in press; (b) H. A. Scheraga, R. A. Scott, G. Vanderkooi, S. J. Leech, K. D. Gibson, T. Ooi, and G. Némethy, in "Conformation of Biopolymers," G. N. Ramachandran, Ed., Academic Press Inc., London, 1967, vol. 1, p 43.

(2) D. W. Jones, *J. Polymer Sci.*, **32**, 371 (1958).

(3) P. DeSantis, E. Giglio, A. M. Liquori, and A. Ripamonti, *ibid.*, **A1**, 1383 (1963).

(4) A. Sarko and R. H. Marchessault, *Science*, **154**, 3757 (1966).

(5) A. Jeanes and R. W. Jones, *J. Am. Chem. Soc.*, **74**, 6116 (1952).

Table I. Characteristics of Corn Amylose and the Triacetate Used in the Sample Preparation

Sample	$\bar{M}_n$ (osmometry)	$\overline{DP}_n$	$[\eta]^{30°}$	I_2/amylose, mg/g	% acetyl
Amylose NRRL, 14SSP	141,000	868	0.76 0.735 (in DMSO)	175–180	...
Amylose triacetate	171,500	592	1.97 (in $CHCl_3$)	...	44.42 44.49

water and were then used to record X-ray fiber diagrams without further treatment.

X-Ray Diffraction Digrams. All diagrams were obtained with a Norelco X-ray diffraction unit equipped with a copper target fine focus tube, in a vacuum flat film camera. Typical experimental conditions were: X-ray unit operated at 35 kv and 20 ma, incident X-ray beam perpendicular to sample surface, film-to-sample distance 5 cm, and pressure in the camera less than 5 mm. Diagrams designed for the measurement of interplanar spacings were taken with a small amount of finely powdered crystalline NaF placed directly on the sample, so that the accurately known 2.319-A spacing of NaF could be used as an internal standard. The spacings were measured on photographic enlargements of the diagrams, and the final values represent an average of at least six films. Diagrams designed for the measurement of intensities were obtained on multiple-film stacks[6] (Kodak No-Screen X-ray film) and the films were developed in fresh developer at recommended conditions. The intensities were determined by visual comparison with a standard scale of intensities. The latter was prepared by recording a series of exposures of the most intense amylose triacetate I reflection and assigning the corresponding exposure time in minutes as the measure of relative intensity to each spot of the series. The "corrected relative integrated intensity" was then obtained from the measured intensity by multiplying the latter by the distance of the reflection from the center of the diagram, thus allowing for the spreading of the spot.[7] The corrected intensities were scaled relative to the most intense reflection which was taken equal to 100. The diffractograms showed no evidence of preferred orientation other than parallel to the fiber axis.

Density. The density of stretched amylose triacetate films was determined by the flotation method in a mixture of a saturated aqueous solution of potassium iodide and pure water at a temperature of 25°. The specific gravity of the solution in which the sample remained floating was determined in a pycnometer.

Computation of Chain Conformations and Theoretical Intensities. The atomic coordinates of all conformations were computed on an IBM 1620 Model II computer, equipped with a 1311 disk drive and 40,000 core memory. A set of FORTRAN programs was written for this purpose so that any desired helical conformation of amylose triacetate could be computed starting with specific bond lengths and angles.[8] Theoretical intensities were calculated with the help of the Shiono "Structure Factor" program.[9]

Results and Discussion

Normally, in X-ray analysis, the structure is solved in logical steps from the unit cell determination to the space group, and finally by the refinement of atomic positions by means of intensity calculations. With fibrous polymers the X-ray data are too meager for such a procedure and many of the steps have to be supplemented by noncrystallographic procedures. In the present study, this took the form of a stereochemical conformational analysis, which complemented the X-ray approach and assisted in its interpretation.

Unit Cell. Although the X-ray fiber diagram clearly indicates hexagonal packing of chains, a hexagonal-shaped unit cell containing one chain did not account for all of the observed reflections. When the unit cell was enlarged to an orthogonal one of twice the volume, all reflections could be indexed, and the match between calculated and observed interplanar spacings was excellent (see Table II). The dimensions of this unit cell are a = 10.87 A, b = 18.83 A, c (fiber axis) = 52.53 A, and its two chains occupy the corner and the center of the ab plane, respectively. Each chain contains 14 glucose triacetate residues per fiber repeat and possesses twofold screw symmetry along the chain axis. Not counting hydrogens, the unit cell encompasses 560 atoms. The theoretical density for this unit cell is 1.24 g/cc, somewhat lower than the experimental density of 1.29 g/cc.

The fact that a unit cell containing two chains had to be adopted to describe a system of hexagonal close packing indicates the presence of two nonequivalent molecules in the crystal. In a crystalline fiber composed of polar chains, it is reasonable to expect that one-half of the chains point in one direction and the other half in the opposite direction. Such chains can crystallize either with all chains parallel in one crystallite, resulting in the fiber containing antiparallel crystallites, or with an antiparallel arrangement of chains in each unit cell resulting in the equivalence of all unit cells and crystallites. Neither possibility could be excluded on the basis of available X-ray data, as the space group, which could have indicated the presence of symmetry relations between the chains, could not be established. Although it may be argued that the parallel case should be excluded on the grounds that parallel hexagonally packed chains would arrange themselves "in phase" relative to one another, resulting in the equivalence of all chains and a true hexagonal unit cell, this argument is not valid here because of the lack of hexagonal or trigonal symmetry in the chain itself. Lack of such symmetry may cause sufficient strain in the "in-phase" packing to force some of the chains out of phase, thus creating nonequivalent parallel chains.

Thus unit cell considerations, coupled with those of molecular transform, afford only an elementary solution to the crystal structure. At this stage, one is confident of the helix parameters and, consequently, the equivalence of monomer positions along the helix axis,[10] the size of the unit cell, and interchain distance. The next objective was a "trial-and-error" structure analysis. The first step in reaching this objective was to determine the most probable conformation of a single isolated chain, on the assumption that *intra*-chain forces play a much larger role in determining polymer structures than do the *inter*-chain forces.[10] (This is a reasonable assumption in the absence of charged groups and of strong attractive forces such as the hydrogen bond.)

Conformation of a Single Helix. At this point in the investigation, an adjustable scale model (2 in./A) of the amylose triacetate molecule was constructed, in order that all the structural variables of the helix be recognized prior to starting a full conformational analysis. The model was to serve also in limiting the range of conformations to be examined, as stereo-

(6) M. J. Buerger, "Crystal-Structure Analysis," John Wiley and Sons, Inc., New York, N. Y., 1960, Chapter 6.
(7) R. E. Franklin and R. G. Gosling, *Acta Cryst.*, 6, 678 (1953).
(8) The computer programs will be described in a separate communication.
(9) R. Shiono, "Structure Factor Program," IBM 1620 General Program Library, No. 8.4.004.
(10) G. Natta and P. Corradini, *Nuovo Cimento Suppl.*, 15 (9) (1960).

Table II. Calculated and Observed *d* Spacings and Intensities (Antiparallel Model) for Amylose Triacetate I[a]

Layer line	Miller indices	*d* spacings, A Calcd	Obsd	Intensities Calcd	Obsd	Layer line	Miller indices	*d* spacings, A Calcd	Obsd	Intensities Calcd	Obsd
0	010			0	0	8	128			0	0
	100			0	0		038			0	0
	020,110	9.414	9.39	102	100		138, 208	4.186	4.16	20	10
	120			0	0		218			0	0
	030			0	0		228, 048	3.825	3.83	13	5
	130, 200	5.435	5.43	9	5		148			0	0
	210			0	0		238			1	0
	220, 040	4.707	4.71	9	5		058			1	0
	140			0	0		308			1	0
	230			0	0		158, 248, 318			1	0
	300			0	0		328			2	0
	050			0	0	9	019			0	0
	150, 240, 310	3.558	3.58	11	10		109			1	0
	320			0	0		029, 119	4.959	4.97	5	12
3	013, 103	12.818, 9.234	9.5–14[b]	27	30[b]		129			4	0
	023, 113	8.290	8.30	21	43		039			1	0
	123, 033	6.592, 5.907	6–8[b]	9	10[b]		139, 209			1	0
	133, 203	5.190	5.18	22	23		219			1	0
	213			0	0		229, 049			0	0
	223, 043	4.545	4.51	12	13		149			0	0
	143			1	0		239			0	0
	233			0	0		059			0	0
	053			0	0		309			0	0
	303			0	0		159, 249, 319			0	0
	153, 243, 313			1	0		329			0	0
	323			0	0	11	0111			0	0
6	016			2	0		1011			0	0
	106	6.816	7–8[b]	6	10[b]		0211, 1111			0	14
	026, 116	6.409	6.42	9	37		1211			0	0
	126, 036	5.521, 5.100	5–6[b]	22	20[b]		0311			0	0
	136, 206	4.617	4.61	15	22		1311, 2011	3.586	3.59	3	12
	216	4.484	4.5[b]	4	10[b]		2111			0	0
	226, 046	4.145	4.14	18	30		2211, 0411			5	4
	146			2	0		1411			1	0
	236			2	0		2311			1	0
	056			0	0	14	0114			0	0
	306			0	0		1014			0	0
	156, 246, 316			4	0		0214, 1114	3.484	3.51	6	12
	326			0	0		1214			0	0
8	018			0	0		0314			0	0
	108			0	0	17	0117			1	0
	028, 118			8	0		1017			0	0
							0217, 1117	2.934	2.94	1	7

[a] Calculated intensities for layer lines 1, 2, 4, 5, 7, 10, 12, 13, 15, 16, 18 were all zero or nearly zero, and no intensities were observed on these layer lines in the X-ray diagram. a = 10.87 A, b = 18.83 A, c (fiber axis) = 52.53 A, $\alpha = \beta = \gamma = 90°$. [b] Diffuse and streaked reflection.

chemically impossible structures could easily be recognized by observation.

On the assumption of structural equivalence of all monomer residues, a given helix could be constructed by fixing the following four parameters: (1) the conformation of the anhydroglucose residue, (2) the conformation of two contiguous anhydroglucose residues relative to one another, (3) the position and conformation of the three acetate groups on each residue, (4) the chirality of the helix. If all of the above factors were varied simultaneously, the resulting conformations would have been too numerous to explore in terms of practical expenditure of computer time. Consequently, a reduction both in the number of factors to be considered simultaneously and the range of variability of each factor was attempted. This was accomplished by the use of the following assumptions and in the following chronological order. First, the internal variability of the anhydroglucose residue was completely eliminated by fixing the bond lengths and angles and the ring conformation. The values are shown in Table III, and they correspond to what

Table III. Bond Parameters Used for the *C1* Anhydroglucopyranose Conformation of the Amylose Triacetate Repeating Unit

Bond	Length, A	Angle	Size
C—C	1.54	All angles about	120°
C—O	1.39	carbonyl C	
C—O (ester)	1.36	All other angles	109° 28′
C=O	1.22		
C—H	1.05		

is generally found in X-ray analysis of carbohydrates.[11] Similarly, such analysis usually reveals a *C1* ring conformation[11] which also coincides with evidence from nmr studies.[12] Thus, for all practical purposes the skeleton of the monomer residue was fixed as a "rigid body," variable only in regard to its position along the helix. This positional variability was considered next, and, as can be seen from the following, it is equivalent to one degree of freedom.

(11) G. A. Jeffrey and R. D. Rosenstein, *Advan. Carbohydrate Chem.*, **19**, 7 (1964).
(12) V. S. R. Rao and J. F. Foster, *J. Phys. Chem.*, **67**, 951 (1963).

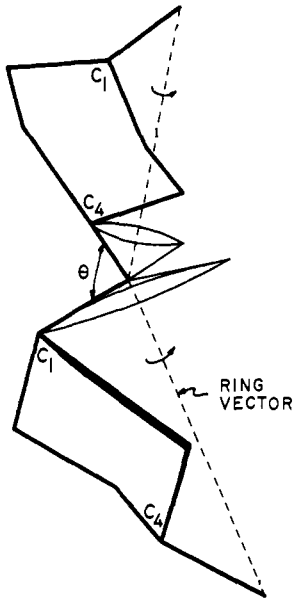

Figure 1. Dependence of the C_1–O_{br}–C_4 bond angle, θ, on the rotation of the anhydroglucose residue about the ring vector. The bond angle is the angle between the surfaces of the two cones of rotation.

From the fiber repeat (52.53 A) and the number of monomer residues per repeat (14), the link point between residues (the bridge oxygen) occurs every 3.752 A (=52.53/14) along the helix axis. Similarly, the angular repeat of bridge oxygens is 77.143° (=3 × 360°/14), measured in the base plane of the helix. These data, together with the end-to-end distance between two consecutive bridge oxygens, completely determine the helix in the sense that each monomer residue can be represented by a vector equal in length to 4.195 A and connecting two successive bridge oxygens. (This vector is henceforth referred to as the *ring vector* of Figure 1.) The only remaining degree of freedom in positioning the ring is in its rotation about this virtual bond. In the absence of restrictions, a residue could theoretically adopt an infinite number of rotational positions; however, in reality there is an important restriction due to the bond angle at the bridge oxygen. As each residue rotates about its ring vector in a synchronous manner (as demanded by the monomer equivalence postulate), the C_1–O_{br} and the C_4–O_{br} bonds each describe a cone of rotation. The angle between the surfaces of the cones constitutes the bond angle, and, since the cones are not coaxial, the bond angle is seen (Figure 1) to vary depending at which point it is measured. When the bond angle is plotted against the rotational position of the ring (*cf.* Figure 2), only a limited range of rotational positions (*ca.* 90°) satisfies the nominal requirement of a 100–120° bond angle.

Observation of the model within the above rotational range showed that for many of the positions several of the distances between nonbonded atoms of two contiguous residues were far shorter than the sum of corresponding atomic (van der Waals) radii.[13] This indicated that the range of rotational positions could be decreased still further. Consequently, when the

(13) V. Sasisekharan in "Collagen," N. Ramanathan, Ed., Interscience Publishers, Inc., New York, N. Y., 1962.

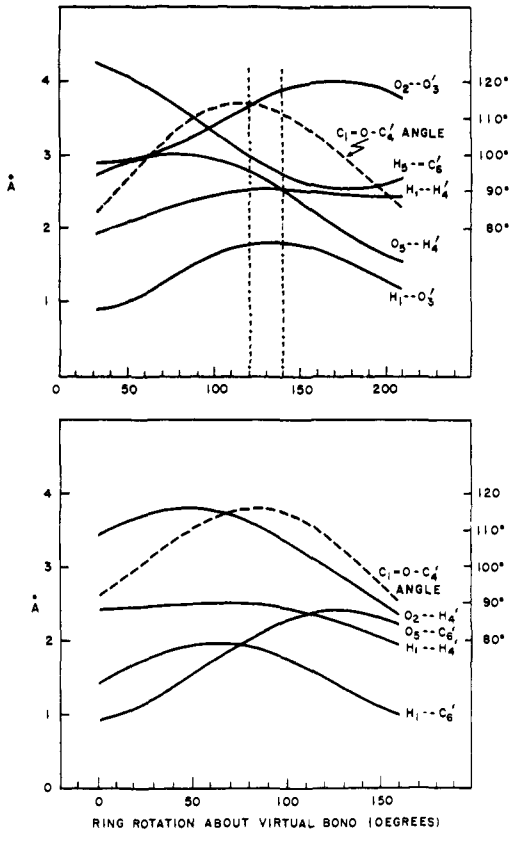

Figure 2. Variation of the C_1–O_{br}–C_4 bond angle (broken line) and the distances between fixed nonbonded atoms (solid lines) of two contiguous residues with rotation of the residue about the ring vector. The zero rotational position for both models is defined by the following atomic fractional coordinates.

Model	Atom	*x/a*	*y/b*	*z/c*
Left-handed	C_1	0.0877	0.0215	0.0766
	O_1	0.1082	−0.0498	0.0714
	O_4	0.1082	0.0498	0.000
Right-handed	C_1	0.0877	0.1042	0.0540
	O_1	0.1082	0.0498	0.0714
	O_4	0.1082	−0.0498	0.000

The area between dotted vertical lines indicates the range of rotational positions relatively free of short nonbonded contacts (distance scale is given on the left, and the angle scale on the right): top, left-handed conformation; bottom, right-handed conformation.

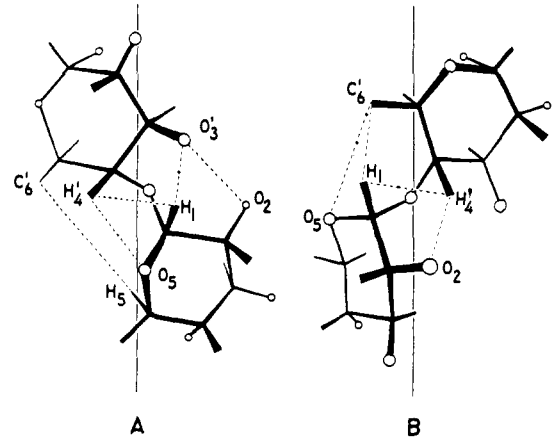

Figure 3. Possible nonbonded interactions between fixed atoms of two continguous residues: A, left-handed conformation; B, right-handed conformation.

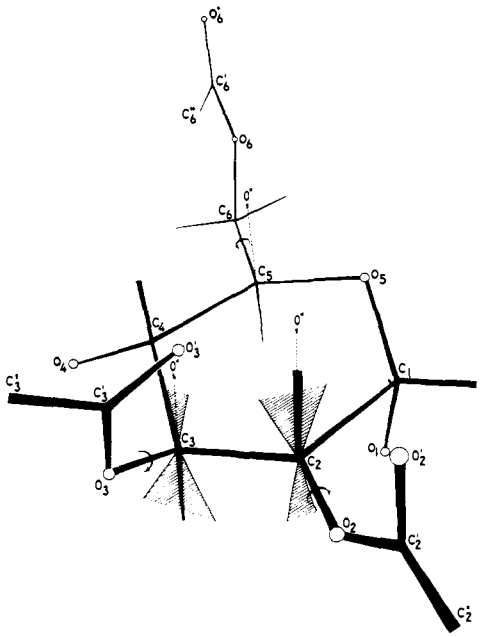

Figure 4. One glucose triacetate residue shown with its acetates in the 0° rotational positions (rotations about the bonds indicated by arrows are positive in the direction of the arrow). The ranges of C_2 and C_3 acetate rotations relatively free of short nonbonded contacts are shown by shaded areas.

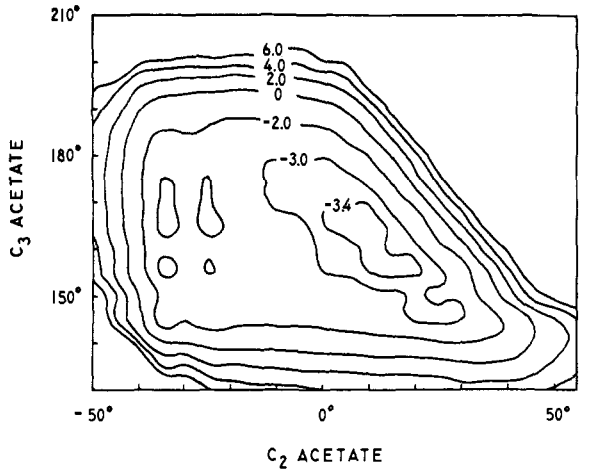

Figure 5. Potential energy of nonbonded interaction as influenced by C_2 and C_3 acetate rotations: left-handed model, C_6 acetate at the 150° position, the glucose triacetate ring at the 130° position. This map shows the lowest potential energy region found in the simultaneous variation of all four parameters.

nonbonded distances between the relevant atoms (shown in Figure 3) were plotted *vs.* the rotational position of the monomer residue, as shown in Figure 2, it could be seen that in both models only a relatively small range of rotational positions (~20°) showed a minimum number of objectionable short contacts between nonbonded atoms. Furthermore, a comparison of the two models showed that the left-handed helix was a more reasonable choice on the basis of only one short contact (H_1- -O_3', short by 0.4–0.6 A) *vs.* two short contacts (H_1- -C_6' and O_2- -H_4', short by 0.5–0.7 A and 0.2–0.4 A, respectively) in the right-handed model. It is quite likely that the short contacts are caused at least in part by erroneous bond parameters used in determining the fixed conformation of the ring and could be alleviated by small adjustments in bond lengths and angles. Even though it would take more adjustment in the right-handed model than in the left-handed one, the right-handed helix was still not excluded from consideration at this point.

The next step in the narrowing of the range of most probable conformations involved the three acetate groups on each ring. This added a great deal of complexity to the problem, as, theoretically, two of the three acetate groups (C_2 and C_3) each possessed two bonds with freedom of rotation and the third acetate (C_6) possessed three such bonds. Simultaneous consideration of all seven variables was clearly too large a task. Fortunately, three of the rotations—those between the ester oxygen and the carbonyl carbon on each acetate—could be eliminated on the basis of the assumption that resonance in the ester link was sufficiently strong to fix the acetate group in a *trans*-planar conformation. Thus, both the C_2 and the C_3 acetate could be considered as rigid bodies able to rotate only about the bond between the ring carbon and the ester oxygen. The C_6 acetate still had an additional variable parameter: rotation about the C_5–C_6 bond. However, simultaneous consideration of four parameters could be handled, and when this was done in a preliminary and qualitative manner with scale models, it was seen that the range of available positions for the acetates could be reduced drastically. For example, both the C_2 and C_3 acetates could be positioned approximately only *cis* or *trans* relative to the respective ring hydrogen (H_2 and H_3), with all other positions excluded owing to very short van der Waals contacts between neighboring acetates. About each *cis* and *trans* position the available rotational range was approximately ±20°. Similarly, of all the positions available through rotation about the C_6–O_6 bond, the least crowded position occurred when the atomic sequence[14] C_6–O_6–C_6'–C_6'' was in a *trans*-planar conformation. Further consideration of both intra- and interchain nonbonded contacts clearly showed that this rotational position could be left entirely invariant. On the other hand, the C_5–C_6 rotation exhibited a comparatively large range of allowable positions. The final rotational ranges thus determined are illustrated in Figure 4.

With the number of rotational parameters reduced to five (rotation of the ring about the virtual bond, three acetate rotations, the handedness of the helix) and the range of the first four defined within relatively narrow limits, it was feasible to consider all variables simultaneously. The immediate objective was to select the most probable conformation for both the left- and the right-handed helix and by comparison of the two to determine the probable chirality of the helix. Rather than continue using the "hard-sphere" method, which excludes conformations solely on the basis of contacts between atoms shorter than the sum of atomic radii, the method was "relaxed" by introducing compressible atoms. The compressibility of an atom is described by an appropriate potential energy function, and such functions determine the contribution of every nonbonded interaction to the potential energy of the mole-

(14) Primed atoms joined by primary valences to unprimed ones refer to atoms in the acetate residue as shown in Figure 4.

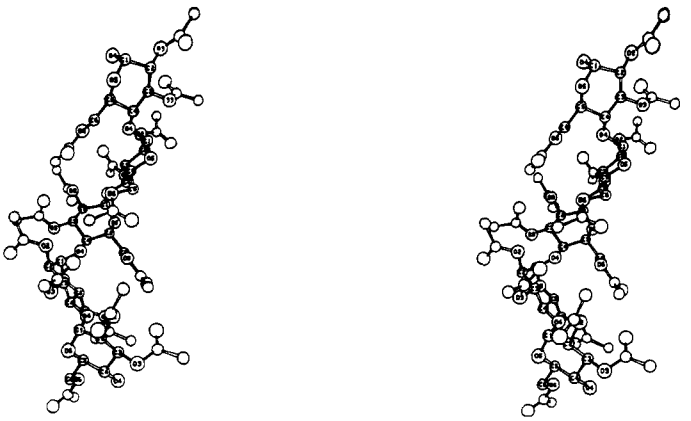

Figure 6. A five-residue segment of the final left-handed conformation of amylose triacetate I. This is a stereoscopic illustration and should be viewed with an appropriate viewer or simply by placing a card between the two drawings so that each of the observer's eyes sees only one image. (An inexpensive stereopicture viewer is manufactured by Stereo Magniscope, Inc., 40-31 81st St., Elmhurst, N. Y. This illustration was drawn with the help of the Oak Ridge Thermal Ellipsoid Program computer program, written by Dr. C. K. Johnson of Oak Ridge National Laboratories.)

cule. The shape of these functions is well known but, unfortunately, the various constants in the analytic expressions for the functions are in question. Thus, the results of the application of these functions must be considered approximations at best. Nevertheless, the use of potential energy functions has correctly predicted the structures of several known synthetic polymers[3] and the α helix of polypeptides,[1] thus lending confidence in their further use. The functions selected were those of Liquori, *et al.*[3,15,16]

The calculations were performed by systematically varying the four positional parameters (within the available ranges as previously defined) and by computing the sum of nonbonded potential energies for all atom pairs whose center-to-center distances were less than 5 A. This was done for both left- and right-handed helices. In this manner, the effects of all nonbonded distances on a given conformation were taken into account. (The nonbonded interactions between the atoms of the carbonyl bond of each acetate and the corresponding ring carbon and its hydrogen were omitted from the summation. This was justified on the basis of evidence[17] that structures containing a double bond are more stable in a *cis* or eclipsed conformation than ordinary nonbonded potential energy functions would indicate. The latter would clearly not be applicable in such cases. At any rate, inclusion of these interactions, calculated with the incorrect potential energy functions, did not materially change the conformation of the acetate groups, indicating that these particular interactions were not of major importance.)

The results were plotted as energy contour maps *vs.* the variation in C_2 and C_3 acetate positions, for given ring and C_6 acetate positions, and clearly indicated that for both helices there was only one sharply defined area of minimum interaction energy. The contour map of the minimum for the left-handed helix is shown in Figure 5, and it is evident that the potential energy rises very sharply with the rotation of the C_3 acetate, and less sharply with the rotation of the C_2 acetate. Although not shown, a sharp rise also occurs with the change in the rotational position of the ring, and to a smaller extent with the change in the position of the C_6 acetate. Thus, only one most probable conformation existed for the left-handed model; the same was found to be true for the right-handed helix. When the minimum energy values of the two helices were compared (-3.5 kcal/mole of residue for the left-handed and 10.8 kcal/mole of residue for the right-handed), it was immediately evident that the left-handed helix is energetically a far more stable conformation that its right-handed counterpart.

Examination of the model for the left-handed helix also indicates several features that are reasonable from an intuitive stereochemical point of view. For example, the rotational position of the ring corresponds with a bridge oxygen bond angle of 113° which is about the most frequently reported angle by carbohydrate crystallographers,[11] and the C_2 and C_3 acetates are positioned so that the carbonyl oxygens and the corresponding ring hydrogens are very nearly eclipsed. A five-residue portion (slightly more than one turn of the helix) of the final conformation is shown in a stereoscopic diagram in Figure 6.

Chain Packing. With the most probable chirality and specific conformation of a single chain determined, the last problem to be settled was that of the polarity of chain packing. Although the unit cell and the pseudo-hexagonal packing of chains has specified the positions of the central axes of the helices, two different chains in a unit cell can still adopt a variety of positions relative to one another by rotation about, and translation along, the helix axes. Therefore, as with the conformation of a single chain, a series of models now consisting of two chains had to be tested

(15) These functions were the only ones available at the start of this work; at the present time, however, several other functions have come into use.[16] A comparison of all known functions reveals a similar energy–distance relation, but significant differences in the absolute energy values at a given interatomic distance.

(16) C. M. Venkatachalam and G. N. Ramachandran in ref 1b, Vol. 1, p 83.

(17) E. A. Walters, *J. Chem. Educ.*, **43**, 134 (1966).

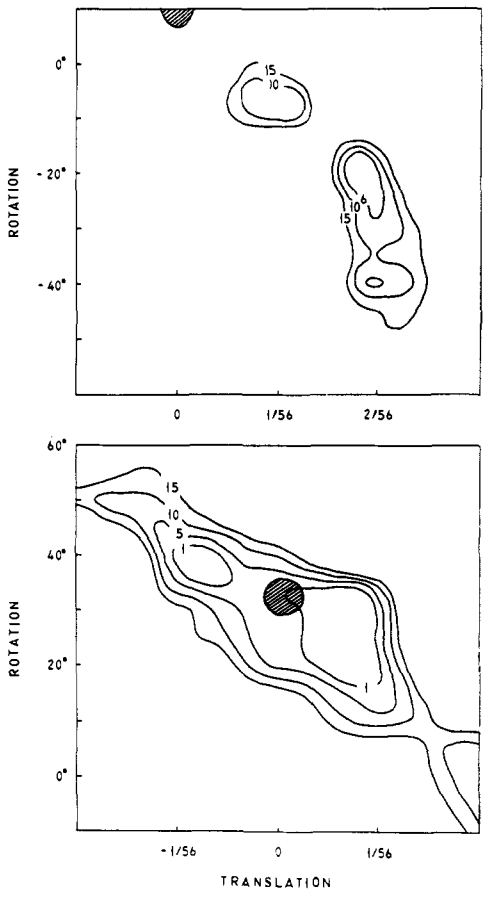

Figure 7. Interchain nonbonded interaction, shown as contours of W, as affected by translational and rotational shifts in the position of the center chain of the unit cell with respect to the corner chain: top, parallel chain arrangement; bottom, antiparallel arrangement. Shaded areas indicate minima in the intensity disagreement index, R_I. The origin position of the corner chain is defined so that the ring vector of the first residue is in the position as specified in the caption of Figure 2. The origin position of the center chain in parallel arrangement is the same, whereas in the antiparallel arrangement it is arrived at by rotation of the corner chain 180° about the y axis of the unit cell.

with regard to a stereochemically sound packing. Each of the two chains was now considered internally invariant, and the models were computed by varying three parameters: (1) polarity of chains (parallel *vs.* antiparallel), (2) relative translational position of the two chains along the helix axes, and (3) rotational position of the chains within each translational position. The total number of models to be considered by the simultaneous variation of the above parameters was relatively small, as the only unique range of translational positions for one chain was within the translational distance equivalent to one monomer residue, *i.e.*, $^1/_{14}$th of the fiber repeat, and similarly, the rotational range was limited to the angle in the base plane of the helix subtended by one residue, or 77.143°.

Since the determination of the most probable packing of chains was really the determination of the final model of the crystal structure, the intensity criterion could be used simultaneously with the stereochemical criterion in the testing of each model. The stereochemical fit was again tested by calculation of nonbonded atomic distances. Since the positions of the hydrogens were not computed in these models, the nonbonded interaction energy could not be obtained as was done in the case of a single chain. Instead, a figure of merit, W, for the packing, was calculated for each model from the following arbitrary weighting function

$$W = \sum_i 40\Delta r_i^4$$

where Δr_i is the difference (in angstroms) between the equilibrium nonbonded interatom distance and the short distance in question. This relation roughly represented the average repulsion energy between different atoms within a distance range slightly less than the equilibrium value. If all the nonbonded atoms were at equilibrium distances, the value for W would be zero, and a shortening of these distances would be signified by a fairly sharp increase in its value. In effect, the use of the above relation amounted to a "relaxing" of the "hard-sphere" approach.

The calculation of theoretical intensities was straightforward: structure factors were obtained for all reflections that could possibly occur in the observed diffraction diagram from the known atomic space coordinates, and the intensity for each reflection was computed from the structure factor by appropriate corrections for the Lorentz, polarization, and multiplicity factors. A temperature factor was not used. As with the stereochemical analysis, again a figure of merit signifying the closeness of fit between the theoretical and observed intensities was applied. Normally, in crystallography, a structure is considered solved when the disagreement index, R, *viz.*

$$R = \frac{\Sigma\left||F_o| - |F_c|\right|}{\Sigma|F_o|}$$

(where F_o is the observed structure factor and F_c is the calculated structure factor) is as low as possible, usually less than 0.10. With fiber diagrams the individual observed structure factors cannot be determined due to an overlap of reflections; hence a disagreement index based on diffraction intensities, R_I, was determined from the intensities, *viz.*

$$R_I = \frac{\Sigma|I_o - I_c|}{\Sigma I_o}$$

The lowest obtainable value for R_I would signify the best match of calculated and observed intensities, and therefore, the best model.

When this analysis was completed for all possible models, both parallel and antiparallel packing, the following results emerged. First, the corner chains had to be definitely fixed in one position, rotated 6° from the arbitrary original position (for the definition of the latter see caption of Figure 7). Only in this position were the crests and troughs of the helical chains "in phase" without significant van der Waals overlaps. Secondly, considering both corner and center chains, the antiparallel packing was stereochemically far more probable than the parallel packing. This was shown by the minimum W value of 0.4 for the former compared to the minimum value of 6.5 for the latter. Contours of W for both packing schemes are shown in Figure 7 as a function of translational and rotational position of the chains. Although

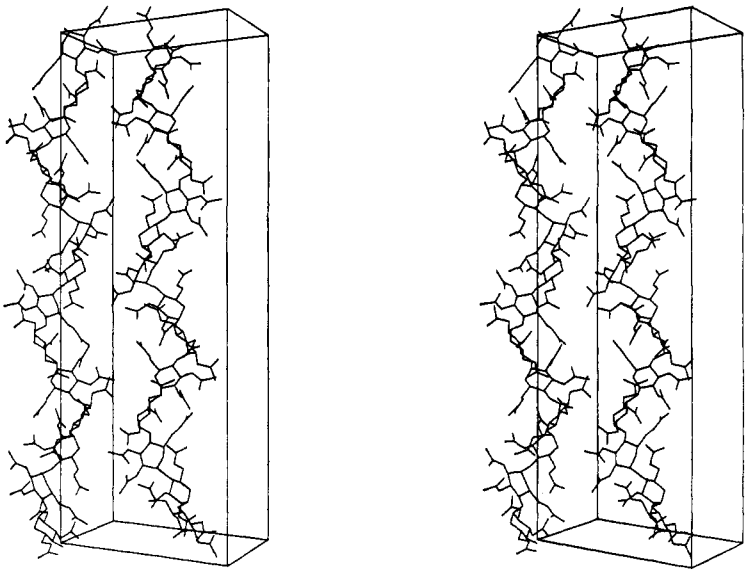

Figure 8. The most probable crystal structure of amylose triacetate I, as shown in a stereoscopic illustration (*cf.* caption of Figure 6). The corner chain of the unit cell is in the "up" direction, and the center chain is in the "down" direction. The rotational position of the corner chain is 6° relative to the origin position (*cf.* caption of Figure 7), and the translational and rotational positions of the center chain are 0 and 30°, respectively, with regard to the corner chain.

there were some short contacts (*e.g.*, 2.765 A) in the antiparallel model (see Table IV), none of them was serious from the standpoint that all involved atoms of acetate groups; thus the resulting minimal amount of strain could easily be relieved by slight rotations or bond angle adjustments. Thirdly, although equal lowest R_I values were obtained for both packing polarities (0.58 in both cases), the minimum value for the antiparallel model coincided with the best stereochemical fit, which was not true in the parallel case (see Figure 7). Both criteria taken together strongly support the antiparallel packing arrangement.

Table IV. Short Interchain Contacts between Nonbonded Atoms in the Antiparallel Model[a]

Atom pair[b]	Distance,[c] A	Atom pair[b]	Distance,[c] A
$1O_6'$–$14C_2''$	3.059	$8O_6'$–$7C_2''$	3.059
$3C_2''$–$12O_6'$	3.018	$10C_2''$–$5O_6'$	3.018
$3C_3''$–$12O_5$	2.915	$10C_3''$–$5O_{14}$	2.915
$4O_5$–$11C_3''$	3.090	$11O_5$–$4C_3''$	3.090
$4O_6'$–$11C_2''$	2.765	$11O_6'$–$4C_2''$	2.765

[a] Each distance appears twice with identical value due to twofold screw symmetry along the chain axis. [b] The number in front of the atom symbol is the sequence number of the monomer residue, counting from the bottom of the unit cell up. For the explanation of atom designations within a monomer residue, refer to Figure 4. [c] Minimum acceptable distance for all following short contacts is 3.15 A.

The values obtained for R_I may need some clarification. Ordinarily, in single crystal analysis, values of the R index as high as observed here signify that the structure is only approximately established and that further refinement should be attempted. In this instance, however, R_I is obtained from experimental values (the observed intensities) which are much less precise than the corresponding quantities from single crystal diagrams. This is especially true of intensities on higher order layer lines. Because of this lack of precision, the small number of reflections present, and the overlap of reflections, more than one structure may yield a minimum value in the R_I index, and the value itself may be rather high. This is precisely what has occurred here, *viz.*, the identical lowest R_I values for both packing models. Owing to the same factors, further refinement of the structure on the basis of diffraction intensities may also be quite unproductive. Nevertheless, a comparison of the observed and calculated intensities for the antiparallel case (shown in Table II) reveals a very satisfactory match, especially for the more reliable intensities on the zero-, third-, and sixth-order layer lines. An R_I factor calculated only for the latter reflections was less than 0.3, indicating an excellent intensity match. This fact, along with the coincidence of the best stereochemical and intensity fits for the antiparallel model, left no doubt that amylose triacetate chains pack preferentially in the antiparallel fashion. The antiparallel unit cell is shown in a stereoscopic diagram in Figure 8, and the fractional coordinates of the atoms of one unit of each chain are given in Table V.

Conclusions

The generally good match between experimental and theoretical intensities and the sound stereochemical packing of the antiparallel model argues to the correctness of the model. The few reflections whose intensities do not match well and the few short van der Waals contacts indicate that some atoms are not in correct positions, but they cannot be off by a significant amount. If the number of reflections observed were larger, a further refinement of the structure could be attempted and would very likely correct the discrepancies; however, in this instance such attempts do not seem worthwhile.

The correctness of the structure also reflects, in general, the validity of the assumptions made in order to decrease the number of models to be considered, and, especially, the sensitivity of the potential energy

Table V. Coordinates of Atoms in One Residue of Each Chain, Antiparallel Model

Corner chain				Center chain			
Atom	*x/a*	*y/b*	*z/c*	Atom	*x/a*	*y/b*	*z/c*
C_1	0.226	−0.060	0.059	C_1	0.260	0.540	0.011
C_2	0.301	0.007	0.054	C_2	0.282	0.620	0.016
C_3	0.227	0.057	0.036	C_3	0.393	0.629	0.034
C_4	0.182	0.015	0.013	C_4	0.380	0.580	0.057
C_5	0.119	−0.053	0.022	C_5	0.348	0.504	0.048
C_6	0.076	−0.096	0.000	C_6	0.332	0.456	0.072
C_2'	0.445	0.037	0.083	C_2'	0.206	0.697	−0.011
C_2''	0.495	0.070	0.107	C_2''	0.207	0.741	−0.036
C_3'	0.278	0.171	0.043	C_3'	0.486	0.734	0.028
C_3''	0.348	0.241	0.037	C_3''	0.512	0.814	0.033
C_6'	−0.081	−0.114	−0.027	C_6'	0.431	0.383	0.099
C_6''	−0.211	−0.102	−0.038	C_6''	0.542	0.342	0.110
O_4	0.098	0.056	0.000	O_4	0.489	0.579	0.071
O_5	0.202	−0.094	0.036	O_5	0.240	0.506	0.034
O_2	0.323	0.042	0.077	O_2	0.304	0.654	−0.006
O_2'	0.515	0.005	0.069	O_2'	0.118	0.700	0.002
O_3	0.302	0.112	0.028	O_3	0.400	0.699	0.042
O_3'	0.200	0.169	0.059	O_3'	0.542	0.703	0.011
O_6	−0.043	−0.076	−0.007	O_6	0.445	0.426	0.078
O_6'	−0.012	−0.157	−0.037	O_6'	0.330	0.376	0.108

method. Evidently, even though the parameters of the potential energy functions may not be accurate, the differences in energy are so large as to be unaffected by small changes in the shape of the functions.

Of particular interest in this study are the conclusions concerning handedness and packing polarity based on the potential energy approach. More often than not, these facts cannot be established from X-ray data alone. A similar approach[18] for an isolated amylose chain did not reveal the same magnitude of preference for one handedness over the other which may reflect a need for including potential energy terms related to intramolecular hydrogen bonding. Such speculation can only be answered by a systematic study of the structure of various polysaccharides. The present approach embodying both experimental X-ray data and potential energy calculations seems to be a powerful method for achieving a complete solution of the solid-state conformation and crystalline packing problem for polymers.

(18) V. S. R. Rao, P. R. Sundararajan, C. Ramakrishnan, and G. N. Ramachandran in ref 1b, Vol. 2, p 721.